Reformulating Multidimensional Population Balances for Predicting Crystal Size and Shape

Zubin B. Kuvadia and Michael F. Doherty
Dept. of Chemical Engineering, University of California Santa Barbara, CA 93106

DOI 10.1002/aic.14167
Published online July 30, 2013 in Wiley Online Library (wileyonlinelibrary.com)

There is a growing interest in predicting and controlling the size and shape of crystalline particles. Multidimensional population balances have been developed to accomplish this task but they suffer from the drawback of needing rate laws for the absolute growth rate for every family of faces that may appear on the crystal surface. Such growth rates are known for only a handful of crystalline materials and prospects are bleak for extending the library of growth rate data. This raises the question of where the surface growth rates for all the families of faces will come from to drive multidimensional population balance engineering technology. One answer is "from first principles." We reformulate multidimensional population balances in terms of relative growth rates and show how to create first principles mechanistic models to calculate these quantities for real molecular crystals as a function of supersaturation. © 2013 American Institute of Chemical Engineers *AIChE J*, 59: 3468-3474, 2013
Keywords: crystal growth (industrial crystallization), crystallization, mathematical modeling

Introduction

In the last decade, there has been a resurgence of interest in modeling crystallization, not seen since the 1960s when Hulburt and Katz[1] published their classic paper, "Some Problems in Particle Technology," in which they introduced the concept of a population balance. Since that time there have been thousands of papers published on this topic using the population balance as a starting point. The literature covers both batch and continuous crystallizers in a variety of designs and configurations, and many other types of solids processing equipment as either stand alone devices or in tandem to form partial or complete process flow sheets.[2–5] Many papers treat optimal operating policies for a huge variety of objectives, as well as control policies, and dynamic effects.[6–12] More recently, there has been a significant effort devoted to the development of real-time *in situ* particle imaging techniques to estimate the population of particle sizes and shapes.[13–17] Concurrently, multidimensional population balances have become the common modeling vehicle for calculating particle size and shape populations.[18–21] The standard model for an isothermal, well-mixed continuous crystallizer has the following form

$$\frac{\partial n}{\partial t} = -G_1 \frac{\partial n}{\partial h_1} - G_2 \frac{\partial n}{\partial h_2} - G_3 \frac{\partial n}{\partial h_3} - \cdots + \frac{n_{\text{in}}}{\tau} - \frac{n}{\tau} \qquad (1)$$

where, n is the crystal-size distribution at time t at any point inside the crystallizer or in the exit stream, n_{in} is crystal-size distribution in the inlet stream to the crystallizer, G_i is the absolute growth rate of the ith crystallographic family of faces on the crystal surface, h_i is the perpendicular distance of the ith face at time t from an origin inside the crystal (see Figure 1), and τ is the residence time for material inside the crystallizer. This population balance is augmented with a solute material balance, an initial condition on n at time $t = 0$, a "regularity" boundary condition at large particle size, an appropriate expression for the nucleation rate (normally assumed to be by secondary nucleation), and a specified value for the parameter τ. The only remaining quantities that must be specified are rate expressions for the growth rates, G_i, for each of the crystal faces. These growth rates have been measured experimentally for several families of faces for a handful of solute–solvent systems, for example, succinic acid grown from aqueous solution,[22] potash alum grown from aqueous solution (see Ma et al., 2008[20] for a compilation of experimental and estimated data), paracetamol grown from aqueous solution,[23] and L-glutamic acid from water.[24,25] The experiments required to obtain the growth rates for all the morphologically important faces are difficult, and few research groups have the wherewithal to obtain them. This may change in the future with the advent of more sophisticated measuring techniques,[16] but for the present we must seek alternative approaches if multidimensional population balances are to be used as a routine engineering tool. This article presents one alternative approach that has the potential to liberate multidimensional population balances from their chains.

Reformulation

Our proposal is to rewrite Eq. 1 in the following equivalent form

This article is dedicated to The Chief, Neal R. Amundson, who pioneered the use of mathematical modeling in chemical engineering. His legacy lives on and gathers strength with each new generation of chemical engineers.

Correspondence concerning this article should be addressed to M. F. Doherty at mfd@engineering.ucsb.edu.

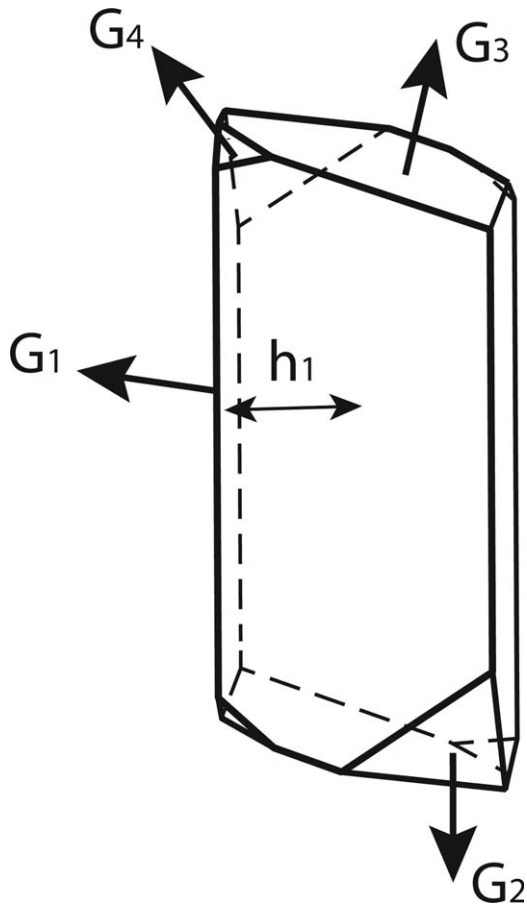

Figure 1. Figure showing growth rates of different families of faces, G_1 to G_4, and the perpendicular distance of the reference face, h_1, from an origin inside the crystal.

$$\frac{\partial n}{\partial t} = -G_1\left(\frac{\partial n}{\partial h_1} + R_2\frac{\partial n}{\partial h_2} + R_3\frac{\partial n}{\partial h_3} + \cdots\right) + \frac{n_{\text{in}}}{\tau} - \frac{n}{\tau} \quad (2)$$

where we have introduced the relative growth rates $R_i = G_i/G_1$, and the family of faces labeled 1 is selected to be the slowest growing face, which is always present on the crystal surface. The other aspects of the formulation accompanying Eq. 1 remain the same. The great advantage of this reformulation is that the relative growth rates can be estimated accurately from first principles using mechanistic growth models that have been perfected in the last few years for solute–solvent molecules of realistic complexity. Thus, in order to solve Eq. 2 it is only necessary to measure the absolute growth rate of a single face – the slowest growing face, and this is no more difficult to obtain than the data necessary to solve one-dimensional (1-D) population balances. Thus, from the data management viewpoint, we have effectively converted the multidimensional population balance into a 1-D population balance but with the added twist that we obtain growth evolution information for all the faces present on the faceted crystal surface. We now show how these relative growth rates can be calculated.

Method to Predict Relative Growth Rates

Mechanistic spiral growth model

Mechanistic growth models predict growth rates for crystal faces by kinetic considerations of events by which growth units incorporate into crystal lattices. Organic crystals are grown mainly at low supersaturations to achieve a high degree of control over the entire crystallization process and ensure stable, uniformly distributed well-faceted crystals by restricting nucleation and avoiding dendritic growth. In the low supersaturation regime where spiral growth is the dominant mechanism for most molecular organics grown in an industrial-like crystallizer, growth will be limited by the kinetics of surface integration processes and not by mass transfer to the surface.[26]

According to the classical Burton, Cabrera and Frank (BCF) model,[27] screw dislocations lead to step edges which flow across the surface due to the addition of solute growth units to result in growth of the surface in its perpendicular direction. The growth rate of a crystal face that is growing by the spiral mechanism can be expressed as

$$G = \frac{hv}{y} \quad (3)$$

where h is the height of the step, v is the step velocity, and y is the interstep distance on the particular terrace/step direction. The BCF model describes the step fronts or edges that form spirals as being composed of multiple kink sites, which are the favorable sites for the incorporation of solute growth units. According to their model, the step velocity is dependent on the number density of kink sites on each step, which in turn is a function of the work required to form the kink sites from a straight step (known as the kink energy). The step height is simply given by geometry (a factor or multiple of interplanar spacing) whereas the interstep distance, y, is a function of energetics and supersaturation.

The traditional approach of assuming a Kossel crystal lattice, a simple cubic lattice with all equal bonds, made the model applicable to centrosymmetric (centric) molecules only (i.e., molecules which have a center of symmetry in their structure). Noncentrosymmetric molecules form complex intermolecular bonding structures in the crystal lattice which pose a set of unique challenges such as multiple growth units and multiple kink types resulting in a nonisotropic driving force on edges in different directions. For about five decades since the BCF model was published, the step velocity was always assumed to be only a function of the number density of kink sites (a natural assumption for Kossel crystals). The concept of kink rate was introduced recently by Chernov[28] and Zhang and Nancollas[29] to account for the nonisotropic driving force. They reasoned that the step velocity must also be directly proportional to the kink rate as well as the kink density, thus

$$v_i \propto a_{p,i}u_i\rho_i \quad (4)$$

where $a_{p,i}$ is the distance of propagation of a step edge, ρ_i is the number density of the kink sites and u_i is the net rate of incorporation into the kink sites.

Recently, Kuvadia and Doherty[30] developed a method and a master equation that can be solved to yield the kink rate for any number of kink sites in series, thus extending the concept to all organic molecular crystals. Kink rate, u_i on an edge i is defined as the net rate of incorporation of solute growth units into different types of kink sites on that particular edge, given by

$$u_i = (\alpha P_k - v_{k+1} P_{k+1})_i \tag{5}$$

where P_k is the probability that the kink site is of the type k, α is the attachment rate of the solute into the kink, and $v_{k,i}$, the detachment rate of the solute from a particular kink type k (which depends on the specific bonds being broken). The above equation represents the two opposing fluxes (corresponding to attachment and detachment) of the solute molecule that is incorporating within the kink site at position k. The probability P_k of each state k can be calculated by setting up a steady-state balance for the influx into and outflux from the state k by the addition and removal of solute molecules into and from the different kink sites (see Figure 2)

$$P_{k-1}\alpha + P_{k+1} v_{k+1} = P_k(\alpha + v_k) \tag{6}$$

where $(k = 1, 2, 3 \ldots n)$ and based on it, a general expression for kink rate on edge i in terms of the attachment rate and detachment rates from different kink sites can be derived

$$u_i = \frac{\left(\alpha^n - v_i^{(n)}\right)}{\sum_{r=1}^{n} \alpha^{n-r} v_i^{(r-1)}} \tag{7}$$

where

$$\begin{aligned}
v_i^{(0)} &= n \\
v_i^{(1)} &= \left(\sum_{k=1}^{n} v_k\right)_i = (v_1 + v_2 + v_3 + \ldots v_n)_i \\
v_i^{(2)} &= \left(\sum_{k=1}^{n} v_k v_{k+1}\right)_i = (v_1 v_2 + v_2 v_3 + \ldots v_n v_1)_i \\
v_i^{(3)} &= \left(\sum_{k=1}^{n} v_k v_{k+1} v_{k+2}\right)_i = (v_1 v_2 v_3 + v_2 v_3 v_4 + \ldots v_n v_1 v_2)_i \\
v_i^{(r-1)} &= \left(\sum_{k=1}^{n} v_k v_{k+1} \vdots v_{k+r-2}\right)_i
\end{aligned} \tag{8}$$

The attachment and detachment rates, α and $v_{k,i}$ can be derived from known rate expressions that are a function of the overall supersaturation and localized bonding structures at each kink site. By inserting values for n, we can generate the kink rate expression for any number of different kink types in series.

Another key concept useful to understand crystal growth of real-complexity systems is the theory of stable and unstable edges,[30] which explains the asymmetric growth spirals on surfaces that are a characteristic of noncentrosymmetric growth units.

Step-by-step methodology to obtain relative growth rates

With the brief background of mechanistic models as described above, a step-by-step methodology to predict relative growth rates of all crystal faces is outlined next. The first step in the methodology is to capture the energetics within the crystal lattice accurately. This is achieved by choosing an appropriate molecular mechanical force field for calculating the nonbonded solid-state interactions within the crystal lattice. The morphology predictions are sensitive to the force field, hence proper care must be taken during force field selection, verifying that the calculated lattice energy values are close to the experimental values, that is, confirming that the overall energetics of the solid are captured. The generalized AMBER force field (GAFF)[31] and the OPLS-AA force field[32] work particularly well with small organic compounds. (Note: The interactions need to be scaled appropriately to account for the solid–fluid interaction in the case of solvent crystallization as described in Snyder and Doherty[33]).

The next step is to identify strong periodic bond chains within the crystal lattice. Hartman and Perdok[34] proposed the concept of periodic bond chains (PBCs) to identify the directions in the lattice which are parallel to the strongest intermolecular interactions. These interactions between the growth units in a lattice are repeated in specific directions which are called PBC vectors. The sum of the interaction energies in each of the PBC directions captures almost 90–95% of the entire lattice energy. Crystal faces can be classified based on the number of PBC vectors that are present within a slice of thickness equal to the interplanar distance d_{hkl}. A face that contains two or more PBCs is called an F face and typically exhibits layer-by-layer growth (other faces grow by rough growth mechanism and disappear quickly). The edges of the growth spirals are parallel to the PBC vectors that are present in that face. Therefore, identifying the

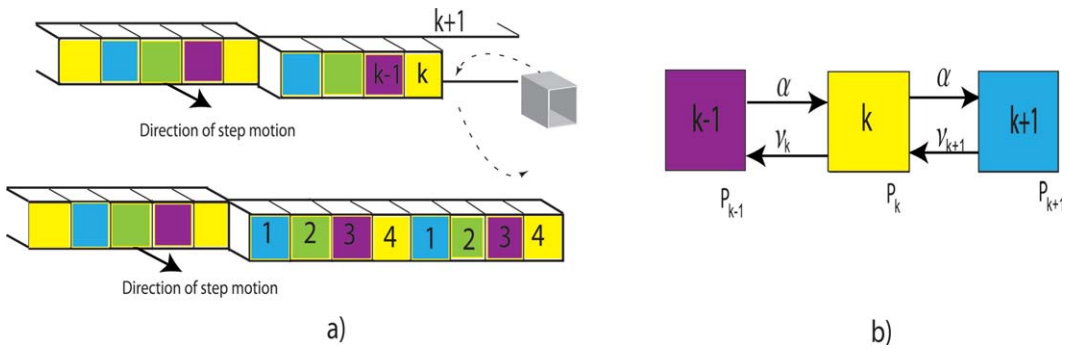

Figure 2. Determination of kink rates.

(a) Incorporation of a growth unit into a kink site and a hypothetical step with four different types of kink sites in series. (b) Steady-state 1-D master equation to find probability of different types of kink sites. [Color figure can be viewed in the online issue, which is available at wileyonlinelibrary.com.]

PBC directions allows the prediction of the shape of the growth spirals formed on each of the F faces present on a crystal surface. On each of these F faces, one does a detailed step velocity calculation using kink densities and kink rates. Based on the crystal geometry and the spiral edge velocity calculation, the relative growth rates of all morphologically important faces can be calculated and the steady-state crystal morphology can be constructed. The entire methodology is summarized pictorially in Figure 3.

This methodology has been validated for various systems of interest such as naphthalene, paracetamol, lovastatin, etc. grown from different solvents and gave excellent agreement of predicted crystal morphology to that observed/measured from experiments. The technique of atomic force microscopy (AFM) scans on crystal faces (*in situ* to measure step velocities or *ex situ* to gain information about terrace widths and step heights) yields immensely valuable information and help improve mechanistic understanding of crystal growth. An AFM scan image of the $\{001\}$ face of a paracetamol crystal grown using water as a solvent (after it reaches steady-state growth) shown in Figure 4a reveals that the spiral shape observed on this face bears a high degree of qualitative agreement with the predicted spiral shape on this face (see Figure 4b). The spiral is an asymmetric polygon and follows the periodic bond chain directions. The symmetric nature of [100] edges (the opposite edges have equal identical interstep distances), and the asymmetric nature of [010] edges, evident by unequal interstep distances of opposite edges is correctly captured. The measured average step height (0.65 nm) from Figure 4c agrees with the interplanar spacing of the $\{001\}$ plane (0.64 nm), thus confirming that the observed steps are monomolecular or elementary in nature.

In general, the relative growth rates of crystal faces remain fairly constant over the range of supersaturations where the spiral growth model applies, as shown in Figure 5[30] based on morphology prediction of paracetamol. Changes in relative growth rates with variation in supersaturation are generally an indication of a change in growth mechanism. This is a very important observation, especially for the application of our multidimensional population balance method as it allows one to directly insert the relative growth rates of the faces into Eq. 2 in the low supersaturation regime in which all crystal faces grow via the spiral mechanism. The absolute growth rate of the slowest face, G_1, in Eq. 2 will depend on the

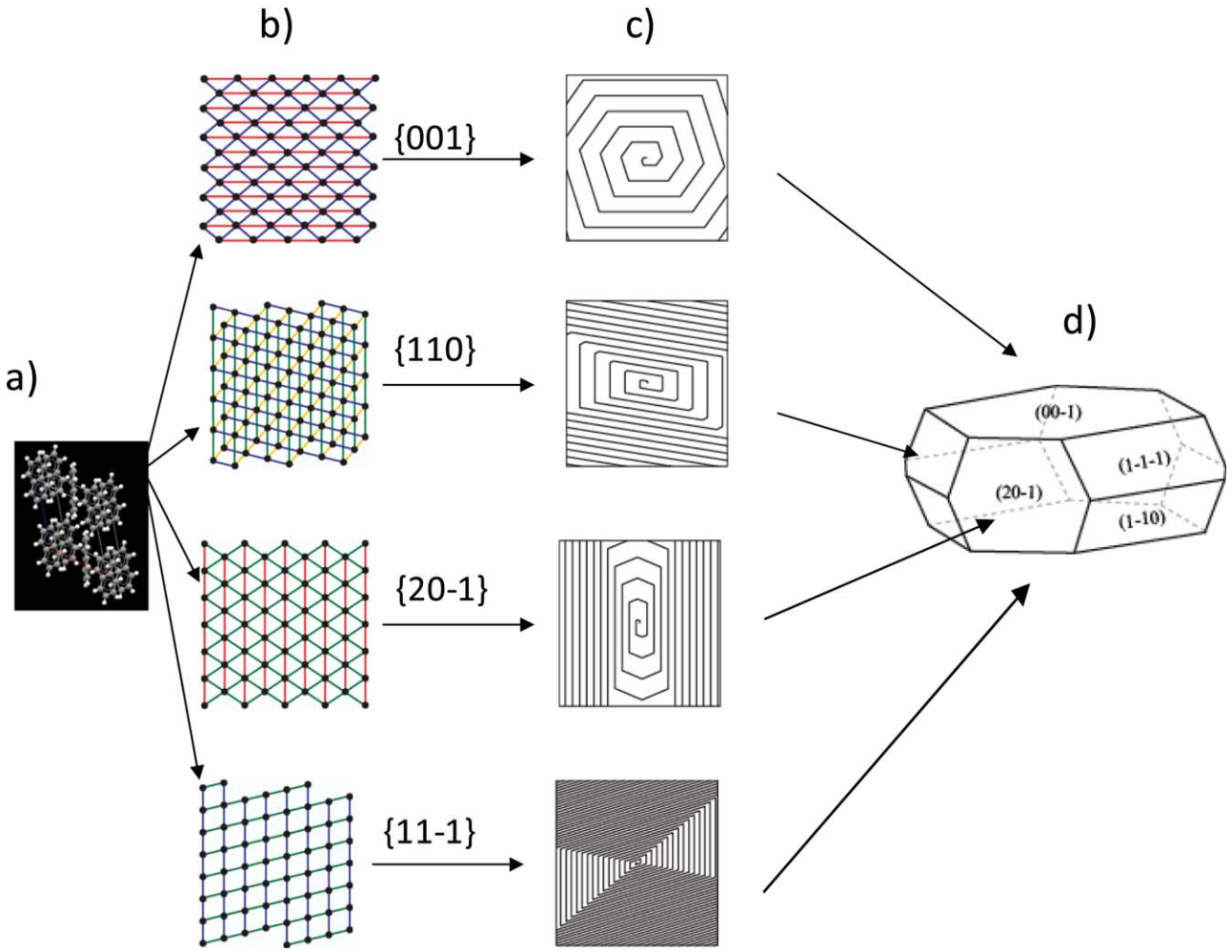

Figure 3. Diagram showing the steps in the overall methodology to predict crystal morphology starting from the unit cell crystal structure.

Image courtesy Michael Lovette (private communication). [Color figure can be viewed in the online issue, which is available at wileyonlinelibrary.com.]

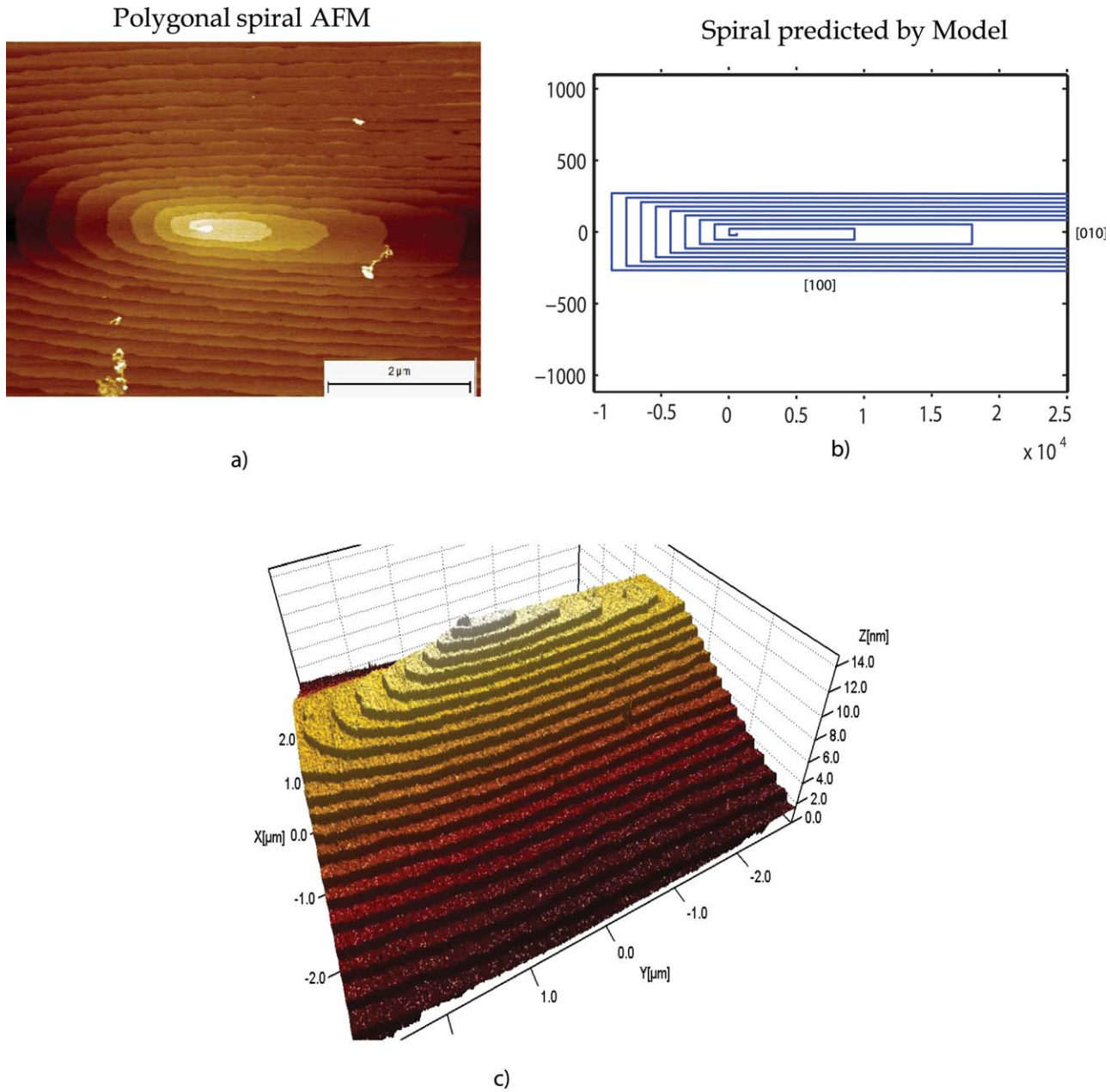

Figure 4. (a) Experimental polygonal spiral observed under an atomic force microscope on the {001} face; (b) the spiral shape predicted by the model; (c) three-dimensional view of the experimental growth spiral on the {001} face, imaged using AFM.

[Color figure can be viewed in the online issue, which is available at wileyonlinelibrary.com.]

supersaturation and an empirical rate expression for this growth rate must be supplied based on experimentally measured data.

Conclusions

This article discusses the formulation of multidimensional population balances and mechanistic methods to obtain relative growth rates of crystal faces for that purpose. We briefly describe mechanistic growth models at low supersaturations, where the spiral growth regime is dominant and the relative growth rates are fairly constant. In scenarios where a mechanism shift from spiral growth to two-dimensional nucleation growth occurs, a more complex treatment along the lines of the supersaturation-dependent morphology model of Lovette and Doherty[35] is warranted. The main advantage of the proposed approach is that it requires only minimal experimental growth rate information, and thus has the potential to become a practical method for modeling size and shape distributions for crystallizing materials. Another noteworthy advantage is that our reformulation method can be combined with any of the existing solution methods for solving multidimensional population balances.[18–21] The growth rate model used by Ma et al.[20] for the three families of faces for potash alum (Eqs. 9–11 in their paper) has constant relative growth rates, thus demonstrating that our approach should work fine

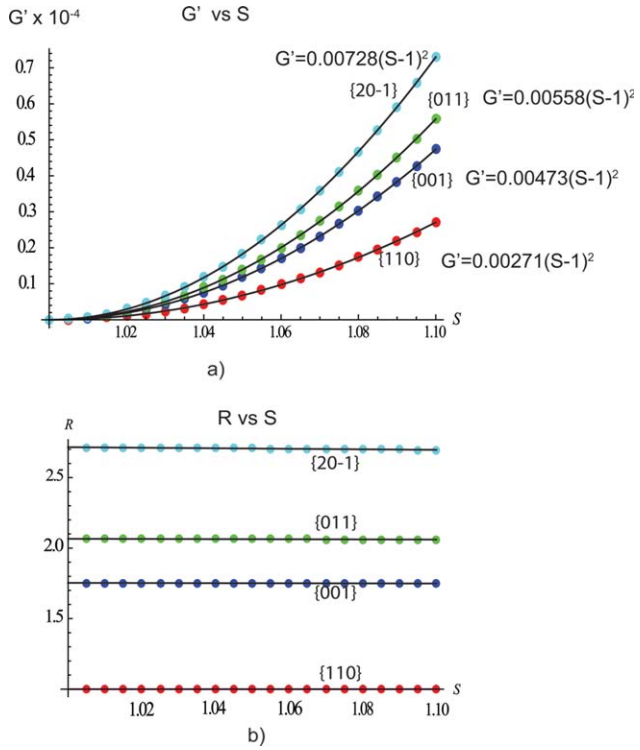

Figure 5. (a) Predicted growth rates (to within a constant multiple) of different faces of paracetamol from aqueous solution using Kuvadia and Doherty[30] model as a function of the supersaturation ($S=C/C_{sat}$) in the low supersaturation regime; (b) relative growth rates of different faces of paracetamol subject to the same conditions.

Different colored dots represent pointwise evaluations of the model, lines represent the best fit polynomial, which is purely quadratic in the relative supersaturation, ($S-1$). [Color figure can be viewed in the online issue, which is available at wileyonlinelibrary.com.]

with existing solution algorithms for solving the population balance equations.

Acknowledgments

The authors wish to thank Stephan Zehrer for his significant assistance in crystal growth experiments of paracetamol grown from aqueous solution and in capturing paracetamol crystal surfaces using AFM. The authors also wish to thank Dr. Michael Lovette for his help with image analysis of AFM snapshots and in generating 3-D images. The authors are grateful for financial support provided by NSF (grant no. CBET-1159746), Abbott Laboratories and Eli Lilly. This work was also partially supported by the MRSEC Program of the National Science Foundation under Award No. DMR 1121053 (use of Materials Research Lab AFM facility).

Literature Cited

1. Hulburt HM, Katz S. Some problems in particle technology: A statistical mechanical formulation. *Chem Eng Sci*. 1964;19:555–574.
2. Randolph AD, Larson MA. Theory of Particulate Processes: Analysis and Techniques of Continuous Crystallization. New York: Academic Press, 1971.
3. Ramkrishna D. Population Balances-Theory and Applications to Particulate Systems in Engineering. San Diego, CA: Academic Press, 2000.
4. Sherwin MB, Shinnar R, Stanley K. Dynamic behavior of the well-mixed isothermal crystallizer. *AIChE J*. 1967;13:1141–1154.
5. Hill PJ, Ng KM. Simulation of solids processes accounting for particle-size distribution. *AIChE J*. 1997;43:715–726.
6. Mullin JW, Nyvlt J. Programmed cooling of batch crystallizers Chem. *Eng. Sci*. 1971;26:369–377.
7. Jones AG. Optimal operation of a batch cooling crystallizer. *Chem. Eng. Sci*. 1974;29:1075–1087.
8. Yu KM, Douglas JM. Self-generated oscillations in continuous crystallizers: Part I. Analytical prediction of the oscillating output *AIChE J*. 1975;21:917–924.
9. Song YH, Douglas JM. Self-generated oscillations in continuous crystallizers: Part II. An experimental study of an isothermal system *AIChE J*. 1975;21:924–930.
10. Rawlings JB, Miller SM, Witkowski WR. Model identification and control of solution crystallization processes: A review. *Ind Eng Chem Res*. 1993;32:1275–1296.
11. Ward JD, Mellichamp DA, Doherty MF. Choosing an operating policy for seeded batch crystallization. *AIChE J*. 2006;52:2046–2054.
12. Nagy ZK, Braatz RD. Advances and new directions in crystallization control. *Annu Rev Chem Biomol Eng*. 2012;3:55–75.
13. Patience DB, Rawlings JB. Particle-shape monitoring and control in crystallization processes. *AIChE J*. 2001;47:2125–2130.
14. Wang X, Anda JCD, Roberts K. Real-time measurement of the growth rates of individual crystal facets using imaging and image analysis: A feasibility study on needle-shaped crystals of L-glutamic Acid. *Chem Eng Res Des*. 2007;85:921–927.
15. Wang XZ, Roberts KJ, Ma C. Crystal growth measurement using 2D and 3D imaging and the perspectives for shape control. *Chem Eng Sci*. 2008;63:1173–1184.
16. Schorsch S, Vetter T, Mazzotti M. Measuring multidimensional particle size distributions during crystallization. *Chem Eng Sci*. 2012; 77:130–142.
17. Borchert C, Sundmacher K. Morphology evolution of crystal populations: Modeling and observation analysis. *Chem Eng Sci*. 2012;70: 87–98.
18. Puel F, Fvotte G, Klein JP. Simulation and analysis of industrial crystallization processes through multidimensional population balance equations. Part 1: A resolution algorithm based on the method of classes. *Chem Eng Sci*. 2003;58:3715–3727.
19. Gunawan R, Fusman I, Braatz RD. High resolution algorithms for multidimensional population balance equations. *AIChE J*. 2004;50: 2738–2749.
20. Ma CY, Wang XZ, Roberts KJ. Morphological population balance for modeling crystal growth in face directions. *AIChE J*. 2008;54: 209–222.
21. Borchert C, Nere N, Ramkrishna D, Voigt A, Sundmacher K. On the prediction of crystal shape distributions in a steady-state continuous crystallizer. *Chem Eng Sci*. 2009;64:686–696.
22. Mullin JW, Whiting MJL. Succinic acid crystal growth rates in aqueous solution. *Ind Eng Chem Fundam*. 1980;19:117–121.
23. Shekunov B, Grant D. In situ optical interferometric studies of the growth and dissolution behavior of paracetamol (Acetaminophen). 1. Growth kinetics. *J. Phys. Chem. B*. 1997;101:3973–3979.
24. Ma CY, Wang XZ. Model identification of crystal facet growth kinetics in morphological population balance modeling of L-glutamic acid crystallization and experimental validation. *Chem Eng Sci*. 2012;70:22–30.
25. Kitamura M, Ishizu T. Growth kinetics and morphological change of polymorphs of L-glutamic acid. *J Cryst Growth*. 2000;209:138–145.
26. Lovette MA, Browning AR, Griffin DW, Sizemore JP, Snyder RC, Doherty MF. Crystal shape engineering. *Ind Eng Chem Res*. 2008; 47:9812–9833.
27. Burton WK, Cabrera N, Frank FC. The growth of crystals and the equilibrium structure of their surfaces. *Phil Trans R. Soc. A*. 1951; 243:299–358.
28. Chernov AA. Modern Crystallography III. Crystal Growth. Berlin: Springer-Verlag, 1984.
29. Zhang J, Nancollas GH. Kink density and rate of step movement during growth and dissolution of an ab crystal in a nonstoichiometric solution. *J Colloid Interface Sci*. 1998;200:131–145.

30. Kuvadia ZB, Doherty MF. Spiral growth model for faceted crystals of non-centrosymmetric organic molecules grown from solution. *Cryst Growth Des*. 2011;11:2780–2802.
31. Cornell WD, Cieplak P, Bayly CI, Gould IR, Merz KM Jr, Ferguson DM, Spellmeyer DC, Fox T, Caldwell JW, Kollman PA. A second generation force field for the simulation of proteins, nucleic acids, and organic molecules. *J Am Chem Soc*. 1995;117:5179–5197.
32. Jorgensen WL, Maxwell DS, Tirado-Rives J. Development and testing of the OPLS all-atom force field on conformational energetics and properties of organic liquids. *J Am Chem Soc*. 1996;118:11225–11236.
33. Snyder RC, Doherty MF. Predicting crystal growth by spiral motion. *Proc R Soc A*. 2009;465:1145–1171.
34. Hartman P, Perdok WG. On the relations between structure and morphology of crystals I. *Acta Crystallogr*. 1955;8:49–52.
35. Lovette MA, Doherty MF. Predictive modeling of supersaturation-dependent crystal shapes. *Cryst Growth Des*. 2012; 12:656–669.

Manuscript received Jan. 22, 2013, and revision received May. 28, 2013.